Indian Journal of Chemistry
Vol. 65, February 2026, pp. 145-163
DOI: 10.56042/ijc.v65i2.25283

Synthesis and spectral studies of some bio-active aryl bis-enones

P Gayathri[†a], P Mayavel[a,b], I Muthuvel[a,c], S Balasundari[a], P Sudha[a], V Usha[d], K Ranganathan[e], V Sathiyendiran[f], B Krishnakumar[†g,h,i], S Rajasri[j], K Veeravelan[k] & G Thirunarayanan*[a]

[a] Department of Chemistry, Annamalai University, Annamalainagar 608 002, Tamil Nadu, India

[b] Department of Chemistry, Government Arts College, Ariyalur 613 204, Tamil Nadu, India

[c] Department of Chemistry, M. R. Government Arts College, Mannargudi 614 001, Tamil Nadu, India

[d] Department of Chemistry, University College of Engineering Panruti, Panruti 607 106, Tamil Nadu, India

[e] Department of Chemistry, P. T. Lee Chengalvaraya Naicker College of Engineering and Technology, Kanchipuram 631 502, Tamil Nadu, India

[f] Department of Chemistry, Sourashtra College, Madurai 625 004, Tamil Nadu, India

[g] Saveetha School of Engineering, Saveetha Institute of Medical and Technical Sciences (SIMATS), Chennai 602 105, Tamil Nadu, India

[h] Department of Civil Engineering, Yeungnam University, Gyeongsan 38541, Republic of Korea

[i] Centre for Research Impact and Outcome, Chitkara University Institute of Engineering and Technology, Chitkara University, Rajpura 140 401, Punjab, India

[j] Department of Chemistry, Raak College of Engineering and Technology, G. N. Palayam, Villiyanur, Puducherry 605 110, India

[k] Department of Science and Humanities, Vel Tech Multi Tech Dr. Rangarajan Dr. Sakunthala Engineering College (Autonomous), Avadi, Chennai 600 055, Tamil Nadu, India

E-mail: drgtnarayanan@gmail.com, thirunarayanan.g.10313@annamalaiuniveristy.ac.in

Received 5 November 2025; accepted (revised) 30 January 2026

Seven series of bis-chalcones have been synthesized *via* the Claisen–Schmidt condensation between various aromatic aldehydes and ketones under conventional heating conditions, utilizing nano fly ash-supported H_3PO_4 as a catalyst in an ethanol medium. The reaction affords yields exceeding 60%. The resulting bis-chalcones have been characterized based on their physical properties, elemental (micro) analyses, and spectroscopic data. The characteristic infrared absorption frequencies (ν, cm^{-1}) corresponding to C=O and νC=C (vinyl) groups, along with the NMR chemical shifts (δ, ppm) of vinyl protons, carbons, and carbonyl carbons in the bis-enones, have been correlated using Hammett substituent constants (σ, σ^+, σ_I, σ_R), field (F) and resonance (R) parameters, as well as Swain-Lupton constants through single and multiple regression analyses. The statistical results have been used to establish quantitative structure-activity relationships (QSAR) for the substituent effects. Molecular docking studies have been further performed to evaluate the protein-ligand interactions of the synthesized bis-chalcones with a target protein. The *in vitro* antimicrobial potential of compounds **8–13** has been determined using the Bauer–Kirby disc diffusion assay, while their antimalarial efficacy has been assessed against *Plasmodium falciparum*.

Keywords: Aryl bis-enones, nano Fly-ash:H_3PO_4, NMR spectra, Hammett correlation, Molecular docking, Bio-activities

Bis-chalcone is indeed an interesting class of compounds, characterized by their α,β-unsaturated carbonyl moieties. This structural feature distinguishes them from typical chalcones, which contain just one such moiety. The presence of two reactive sites can lead to enhanced biological activities and potential applications in medicinal chemistry[1]. Dibenzalacetone derivatives, such as those discussed in this study, are often collectively referred to as dibenzalacetone compounds and areknown for their diverse biological activities[2]. Chalcones, which serve as the core structural motif in these compounds, are aromatic ketones that act as key intermediates in the biosynthesis of a wide array of bioactive molecules. The presence of a reactive α,β-unsaturated keto functional in chalcones is primarily responsible for their pronounced antimicrobial properties. Enhancing interest has been directed toward the synthesis of α,α′-bis(substituted benzylidene) cycloalkanones commonly known as dibenzalacetone derivatives due to their versatile reactivity and biological significance[3,4]. Bis-chalcones, which feature two chalcone moieties within a single molecular framework[5], have recently garnered attention for their synthetic utility and promising pharmacological potential[6]. These scaffolds are not only important intermediates in the synthesis of various heterocyclic systems but also serve

† These authors contributed equally to this work.

as precursors to flavonoids, a class of naturally abundant plant compounds. The electrophilic nature of their α,β-unsaturated ketone functionality renders bis-chalcones reactive toward a range of nucleophilic species, enabling the formation of five-, six-, and seven-membered heterocycles such as pyrazoles[8], isoxazoles[9], thiazoles[10], indoles[11], pyrimidines, and thiazines[12]. Dibenzalacetone analogues are typically synthesized *via* aldol condensation reactions between benzaldehyde (or its derivatives) and acetone[7], where acetone's two α-hydrogens facilitate a 2:1 reaction stoichiometry[13]. Due to their ability to act as Michael acceptors, bis-chalcones also readily participate in a range of conjugate addition reactions, including alkylation and halogenation, further expanding their synthetic versatility. Bis-chalcones are preferred structures in organic synthesis because of their strong reactivity, utility in medicinal chemistry, and expression of numerous significant pharmacological actions[14]. The double bond in these compounds can utilize either *(Z)* or *(E)* configurations, with the *(E)* isomer generally being more thermodynamically stable and thus typically prevalent[15]. Nevertheless, in certain biological contexts, the *(Z)* isomer has been found to exhibit enhanced activity toward specific targets, making the interconversion between isomers often induced by light exposure an important consideration[16]. The synthesis of bis-chalcones is highly sensitive to the reaction environment. A contemporary and environmentally friendly approach involves solvent-free synthesis, aligning with principles of green chemistry[17]. Among the various synthetic methodologies applicable to chalcone derivatives[18], the Claisen–Schmidt condensation is quite extensively used, alongside other notable reactions such as the Wittig reaction, Suzuki coupling, and Mizoroki–Heck reactions. Both acidic and basic catalysts have been successfully employed for these transformations. While homogeneous catalysts are predominantly used in Claisen–Schmidt reactions, heterogeneous catalysis has also yielded promising results[19]. Additionally, although less commonly applied to bis-chalcone synthesis, catalysts like sulfuric acid (H_2SO_4) and thionyl chloride ($SOCl_2$) have demonstrated effectiveness in certain cases[20]. Bis-chalcones not only participate in various chemical transformations but also serve as key intermediates in the synthesis of a broad array of heterocyclic systems. Numerous studies have documented the preparation of bis-chalcone derivatives through condensation of aryl ketones with aromatic aldehydes using suitable condensing agents, emphasizing their importance both as synthetic intermediates and for their diverse biological activities such as anti-inflammatory[21], anti-malarial[22], antiviral[23], anticancer activities[24], antibacterial[25], and antioxidant[26], anti–fungal[27], antidiabetic[28] and anti-HIV agents[29]. Spectral correlation has proved for the prediction of ground state configuration of s-*cis*, s-*trans*, *E* and *Z* geometries of various enol-enone systems[30]. Molecular docking study involves the study of binding interactions of organic substrates with specific proteins. The novel compounds demonstrated strong binding affinities with target proteins 3ERT, 1M17, 1SA0, and 5XDL, as evidenced by molecular docking studies, which were further substantiated through molecular dynamics simulations[25,31]. This research involved the strategic design of innovative derivatives utilizing natural product-based scaffolds, such as anthracene and bis-chalcones, using molecular docking methodologies. The interaction of these compounds with the breast cancer-related protein 3ERT revealed enhanced solubility and reduced interaction energy, highlighting their promise as potential anticancer agents[32]. Bis-chalcones are also recognized for their notable antimalarial efficacy, particularly against *Plasmodium falciparum*, the most lethal of the four *Plasmodium* species affecting humans and a major contributor to malaria-related deaths[22,33]. A comprehensive understanding of the molecular mechanisms behind successful antimalarial agents is essential for future drug discovery efforts[22,33,34]. A literature review indicates a lack of studies examining the spectral characteristics, molecular docking performance, and biological activities including antimicrobial and antimalarial of the synthesized bis-chalcones presented in this work. Therefore, the authors have undertaken the synthesis and evaluation of these compounds to assess their spectral profiles and explore their therapeutic potential.

Results and Discussion

Chemistry

In this study, authors synthesized seven series of aryl bis chalcones using acetone, aryl ketones, di-ketones, aldehydes and di-aldehydes with nano fly-ash:H_3PO_4 as catalyst employing conventional heating method. The condensation reaction afforded bis-chalcones in yields exceeding 75%. Here the electron-donating substitutes in aldehydes or ketones gave more yields than the electron-withdrawing

substituents. This reaction proceeds *via* the well-established acid-catalyzed Claisen–Schmidt condensation pathway. The first step is the formation of enol-enone by protonation of carbonyl oxygen and loss of one α-hydrogen atom of ketone then it leads to formation of carbanions. Second step is the attack of carbanion to carbonyl carbon of aldehydes to form oxide ions. The third step is the oxide ions protonated. In the fourth step, dehydration *via* β-elimination yields the chalcone, and repetition of these steps affords the corresponding bis-enones. The mechanistic path way of the bis-chalcones (1*E*,4*E*)-1,5-bis(substituted phenyl)penta-1,4-dien-3-ones; **1-13**) formation was illustrated in Scheme 1. The remaining bis-enone (**14-59**) formation mechanistic pathway is provided in the Supplementary Information as Scheme S1-S6 (Supplementary Information, Scheme S1-S6).

In this condensation reaction, the influence of catalyst concentration on the formation of bis-enone (**1**) studied by altering the catalyst quantity from 0.1 g to 1 g. An increase in catalysts loading up to 0.5 g resulted in a corresponding rise in product yield from 33% to 86%. However, further increases beyond 0.5 g did not produce any significant improvement in yield. Fig. 1 depicts how catalyst concentration affects the condensation reaction.

The effect of different solvents on the yield of bis-enone (**1**) was also examined by performing the condensation reaction in various media, including acetonitrile, dichloromethane, dioxane, ethanol,

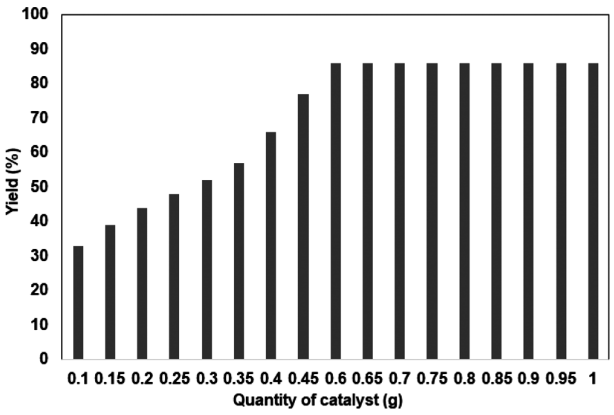

Fig. 1 — Effect of catalyst and the yield of bis-enone (**1**)

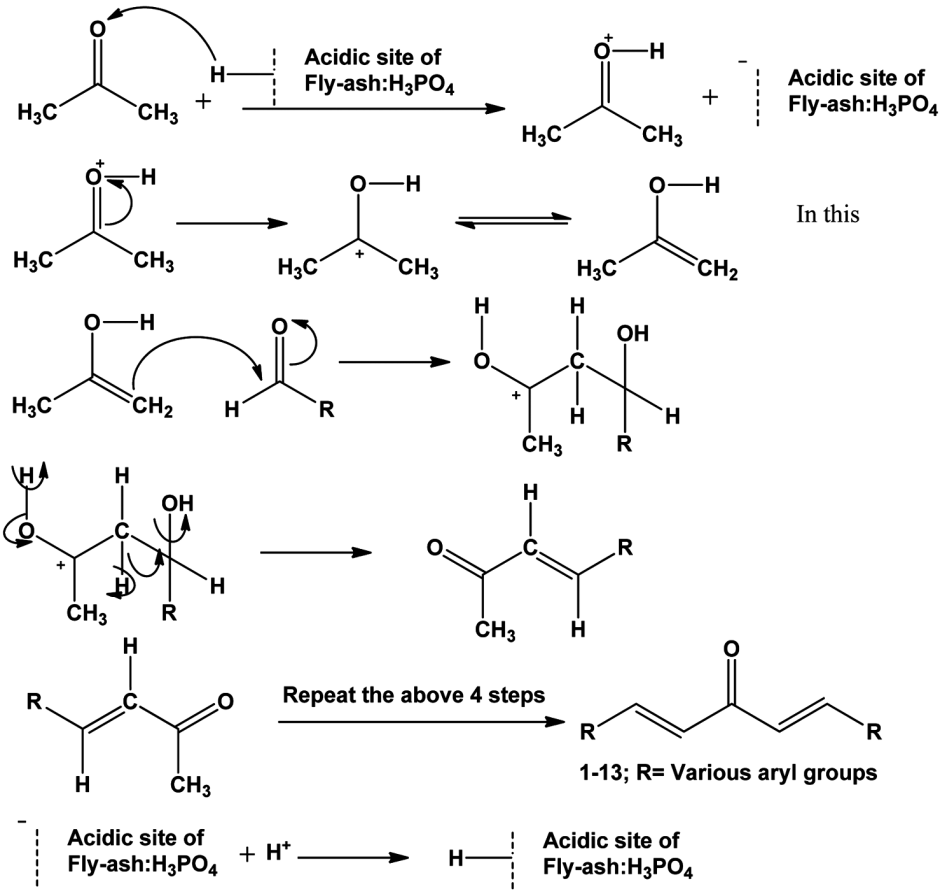

Scheme 1 — The mechanistic pathway of synthesis of bis-enones **1-13**

Table 1 — Effect of solvents on the yields of bis-enones **1-13**

Solvent Entry	R	ACN	DCM	DO	EtOH	MeOH	2-PROP	THF
1	Ph	33	46	52	82	75	73	61
2	4-BrPh	42	40	49	75	66	67	58
3	2-ClPh	40	43	48	80	67	64	59
4	4-ClPh	38	42	46	84	68	69	57
5	4-FPh	36	34	48	72	62	61	49
6	4-OCH_3Ph	53	51	56	86	79	76	66
7	4-CH_3Ph	48	48	54	84	72	72	63
8	9-Anthracene	38	42	49	71	63	51	51
9	4-BiPh	40	40	50	79	58	54	49
10	2,3-Cl_2Ph	46	39	44	80	68	64	57
11	2-Ferrocene	41	38	40	73	52	59	51
12	3-OCH_3Ph	50	53	55	81	74	75	63
13	1-Pyrene	39	39	41	79	55	51	58

ACN: Acetonitrile; DCM: Dichloromethane; DO: Dioxane; EtOH: Ethanol; MeOH: Methanol; 2-PROP: 2-Propanol; THF: Tetrahydrofuran

methanol, and tetrahydrofuran. Among these, ethanol proved to be the most effective solvent, affording the highest product yield, whereas acetonitrile resulted in the lowest yield. The solvent's effect of variation on the condensation reaction is summarized in Table 1.

Spectral correlation study

From the infrared spectra, the characteristic stretching frequencies and the NMR chemical shifts of the synthesized single substituted bis-chalcones [(1*E*,4*E*)-1,5-bis(substituted phenyl)penta- 1,4-dien-3-ones; **1-7** and **13**), (2*E*,6*E*)-2,6-bis(substituted benzylidene) cyclohexanones; **14-22**) and (2*E*,6*E*)-2,6-bis (substituted benzylidene) cyclopentanones; **23-29**)] the assigned data are summarized in Table 2. The measured spectral frequencies (ν, cm^{-1} and δ, ppm) were statistically correlated with Hammett constants and Swain–Lupton parameters (F and R) through single and multiple regression analyses[35-39].

Infrared spectral correlation

The value of infrared stretching frequencies (ν, cm^{-1}) of the synthesized bis-chalcones are listed in Table 2. The correlation of these data was performed using the Hammett equation, as shown below.

$$\nu = \rho\sigma + \nu_o \quad \ldots (1)$$

where ν represents the frequency of the parent member of the series.

The νC=O and νC=C (cm^{-1}) stretching frequencies of the bis-chalcones, (1*E*,4*E*)-1,5-bis(substituted phenyl) penta-1,4-dien-3-ones, exhibited good correlations with the Hammett substituent constants (σ, σ^+, σ_R) and resonance parameter (R), except the methyl and methoxy substituents (Supplementary Information, Table S1). Whether included these substituents in the regression, they lead to failed the correlation. All correlation of CO and resonance component correlation of C=C shows negative ρ values obtained for the νC=C stretches suggest a reversal of substituent effects in all systems. Lack of correlation with other parameters arises from the negligible influence of polar, field, and inductive factors, rendering them ineffective in predicting variations in νC=O and νC=C bands. This observation aligns with the conjugative structure depicted in Fig. 2.

The single parameter correlations of νC=O (cm^{-1}) frequencies of (2*E*,6*E*)-2,6-bis(substituted benzylidene) cyclohexanone derivatives showed acceptable correlation coefficients through Hammett substituent constants. Likewise, the νC=C (cm^{-1}) bands of the bis-chalcones correlated well with resonance and field parameters, except for the bromo-substituted compound. If this bromo substituent will include the regression, it directed to fails the correlation. The remaining correlation was failed. The absence of correlation arises from the limited contribution of polar and inductive effects, with the frequencies mainly governed by resonance–conjugative interactions, as exposed in Fig. 3.

Correlations of νC=O and νC=C (cm^{-1}) frequencies of (2*E*,6*E*)-2,6-bis(substituted benzylidene) cyclo-pentanones with Hammett substituent constants produced satisfactory correlation coefficients except parent, methoxy and methyl substituents. Some of the correlation produced negative ρ values. These

Table 2 — The characteristic infrared stretching frequencies (ν, cm^{-1}) and the ^1H and ^{13}C NMR chemical shifts (δ, ppm) of the synthesized bis chalcones (**1-7, 12, 14-22** and **23-29**)

Entry	Substt.	IR (ν, cm^{-1})		^1H and ^{13}C NMR (δ, ppm)				
		$C=O_{(s\text{-}cis,\ cis)}$	C=C	H_α	H_β	C=O	C_α	C_β
		(1*E*,4*E*)-1,5-Bis(substituted phenyl)penta-1,4-dien-3-ones						
1	H	1654	1571	7.11	7.79	188.92	125.45	143.32
2	4-Br	1652	1562	7.66	7.55	188.50	129.90	142.30
3	2-Cl	1646	1563	8.13	7.07	188.80	127.20	139.60
4	4-Cl	1650	1589	6.68	7.67	188.40	127.70	141.20
5	4-F	1650	1582	7.7	6.99	188.50	125.03	142.02
6	3-OCH_3	1660	1621	6.6	7.69	198.41	123.49	143.25
7	4-OCH_3	1687	1584	6.94	6.91	188.90	127.50	142.70
12	4-CH_3	1646	1565	7.69	7.55	188.90	127.50	142.70
		(1*E*,4*E*)-1,5-Bis(substituted phenyl)penta-1,4-dien-3-ones						
14	H	1654	1571	7.73	7.07	189.01	128.50	143.30
15	4-Br	1652	1562	7.66	7.55	188.50	129.90	142.30
16	2-Cl	1646	1563	8.13	7.07	188.80	127.20	139.60
17	4-Cl	1650	1589	6.68	7.67	188.40	127.70	141.20
18	4-F	1650	1582	7.7	6.99	188.50	125.03	142.02
19	3-OCH_3	1660	1621	6.6	7.69	198.41	123.49	143.25
20	4-OCH_3	1687	1584	6.94	6.91	188.90	127.50	142.70
21	4-CH_3	1646	1565	7.69	7.55	188.90	127.50	142.70
22	4-NO_2	1691	1691	–	7.8	188.32	126.78	135.20
		(2*E*,6*E*)-2,6-Bis(substituted benzylidene)cyclopentanones						
23	H	1686	1597	–	7.65	196.62	128.80	137.30
24	4-Br	1697	1583	–	7.58	196.10	124.00	137.50
25	2-Cl	1695	1585	–	7.58	195.50	126.60	139.30
26	4-Cl	1694	1584	–	7.55	196.25	132.13	136.80
27	4-F	1695	1586	–	7.56	196.25	132.13	136.80
28	4-OCH_3	1698	1585	–	7.65	196.24	128.80	133.00
29	4-CH_3	1686	1588	–	7.66	196.26	129.65	139.89

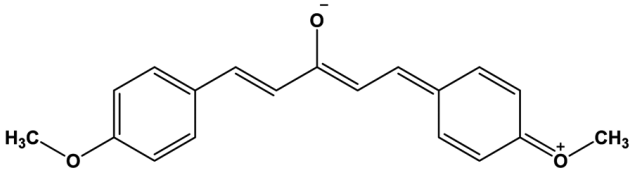

Fig. 2 — The resonance-conjugative structure of bis-enone **7**

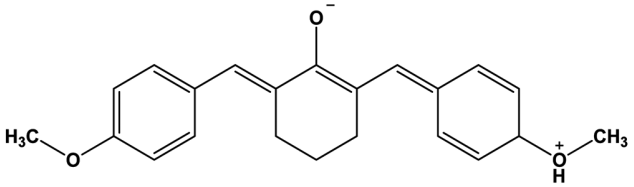

Fig. 3 — The resonance - conjugative structure of methoxy substituted bis-enone

observations suggest the presence of a reversed electronic effect in the system.

Multiple regression analysis produced satisfactory correlations of the spectral frequencies by Swain–Lupton's field (F) and resonance (R) parameters[39], as summarized in equations (2–13). (1*E*,4*E*)-1,5-Bis(substituted phenyl)penta-1,4-dien-3-ones

$\nu C{=}O\ (cm^{-1}) = 1650.26\ (\pm 9.21) - 24.82\ (\pm 25.14)\ \sigma_I - 50.96\ (\pm 32.75)\ \sigma_R$ …(2)

(R =0.927, n = 8, *P* >95%)

$\nu C{=}O\ (cm^{-1}) = 1649.85\ (\pm 8.01) - 30.26\ (\pm 21.85)\ F - 49.39\ (\pm 23.73)\ R$ …(3)

(R =0.936, n = 8, *P* >98%)

$\nu C{=}C\ (cm^{-1}) = 1567.26\ (\pm 12.26) - 29.59\ (\pm 34.24)\ \sigma_I - 84.54 (\pm 44.61)\ \sigma_R$ …(4)

(R =0.967, n = 8, *P* >96%)

$\nu C{=}C\ (cm^{-1}) = 1566.37\ (\pm 12.06) - 26.19\ (\pm 32.92)\ F - 68.75\ (\pm 35.74)\ R$ …(5)

(R = 0.957, n = 8, *P* > 96%)

(2*E*,6*E*)-2,6-Bis(substituted benzylidene) cyclohexanones

$\nu C{=}O\ (cm^{-1}) = 1667.32\ (\pm 26.150) - 57.94\ (\pm 56.082)\ \sigma_I - 59.44\ (\pm 63.007)\ \sigma_R$ …(6)

(R =0.927, n = 9, *P* > 98%)

$\nu C{=}O\ (cm^{-1}) = 1671.13\ (\pm 26.36) - 46.80\ (\pm 55.85)\ F - 47.88\ (\pm 49.901)\ R$ …(7)

(R =0.951, n = 9, *P* >95%)

$\nu C{=}C\ (cm^{-1}) = 1587.8\ (\pm 22.19) - 31.37\ (\pm 47.60)\ \sigma_I - 6.931\ (\pm 53.477)\ \sigma_R$ …(8)

(R =0.967, n = 9, *P* > 96%)

$\nu C{=}C\ (cm^{-1}) = 1590.42\ (\pm 21.95) - 24.205\ (\pm 46.502)\ F - 7.438\ (\pm 41.547)\ R$ …(9)

(R = 0.957, n = 9, *P* > 98%)

(2*E*,6*E*)-2,6-Bis(substituted benzylidene) cyclopentanones

$\nu C{=}O\ (cm^{-1}) = 1686.75\ (\pm 2.092) - 13.390\ (\pm 6.228)\ \sigma_I - 9.212\ (\pm 8.763)\ \sigma_R$ …(10)

(R =0.927, n = 9, *P* >98%)

$\nu C{=}O\ (cm^{-1}) = 1687.55\ (\pm 2.093) - 2.583\ (\pm 10.856)\ F - 7.749\ (\pm 6.467) R$ …(11)

(R =0.966, n = 9, *P* >95%)

$\nu C{=}C\ (cm^{-1}) = 1591.77\ (\pm 2.748) - 12.546\ (\pm 8.177)\ \sigma_I - 4.509\ (\pm 11.507)\ \sigma_R$ …(12)

(R =0.967, n = 9, *P* > 96%)

$\nu C{=}C\ (cm^{-1}) = 1591.12\ (\pm 2.996) - 10.133\ (\pm 8.986)\ F + 3.146\ (\pm 10.830)\ R$ …(13)

(R = 0.957, n = 9, *P* >94%)

NMR spectral correlation study

The NMR correlation study utilized the Hammett equation, as given in equation 2.

$$\delta = \rho\sigma + \delta_o \quad \ldots(14)$$

where δ_o is the chemical shift (ppm) for the parent member of the series.

^{1}H NMR spectral correlation study

The results of the single regression statistical analysis between the proton chemical shifts of bis-chalcones and the Hammett substituent constants, as well as the F and R parameters, are provided in the Supplementary Information (Supplementary Information, Table S1). The inductive influence of substituents in (1*E*,4*E*)-1,5-bis(substituted phenyl) penta-1,4-dien-3-ones exhibited satisfactory correlation only for the H_α proton chemical shifts (ppm), except for hydrogen and methyl substituents, which displayed negative ρ values. The remaining substituent correlations failed to produce significant correlation coefficients. Similarly, the correlations of H_β proton chemical shifts (ppm) with the Hammett substituent constants, F and R parameters were unsatisfactory. This behaviour may be attributed to the previously discussed factors and is consistent by the resonance–conjugative structural model exposed in Fig. 3.

The correlation analysis of H_β chemical shifts (ppm) for (2*E*,6*E*)-2,6-bis(substituted benzylidene) cyclo-hexanones exhibited satisfactory correlation coefficients using the Hammett substituent constants, as well as the F and R parameters, except for hydrogen substituents in the σ_I and F parameters. All correlations displayed positive ρ values, with the exception of the F parameter, which showed a negative trend.

Likewise, the H_β chemical shifts (ppm) of (2*E*,6*E*)-2,6-bis(substituted benzylidene) cyclo-pentanones exhibited satisfactory correlation coefficients with the Hammett substituent constants, along with the F and R parameters, except for the methoxy substituent in the σ_R constant. The correlations involving resonance components produced positive ρ values, indicating that ordinary substituent effects were operative throughout the system.

All chemical shifts (δ, ppm) of H_α and H_β proton of the aforementioned bis-enones exhibited satisfactory correlation coefficients with the Swain–Lupton constants, as well as the F and R parameters[39], in the multi-regression analysis. The corresponding multiple regression equations are presented in equations (15–22).

(1*E*,4*E*)-1,5-Bis(substituted phenyl)penta-1,4-dien-3-ones

$\delta H_\alpha(ppm) = 7.606\ (\pm 0.434) + 0.571\ (\pm 1.184)\ \sigma_I - 1.538\ (\pm 1.543)\ \sigma_R$ …(15)
(R=0.978, n = 8, *P* >92%)

$\delta H_\alpha(ppm) = 7.613\ (\pm 0.401) + 0.798\ (\pm 1.096)\ F - 1.522\ (\pm 1.190)\ R$ …(16)

(R= 0.989, n = 8, *P* >95%)

$\delta H_\beta(ppm) = 7.422\ (\pm 0.268) + 0.075\ (\pm 0.731)\ \sigma_I - 0.529\ (\pm 0.953)\ \sigma_R$ …(17)
(R= 0.967, n = 8, *P* >98%)

$\delta H_\beta(ppm) = 7.416\ (\pm 0.264) + 0.095\ (\pm 0.721)\ F - 0.227\ (\pm 0.783)\ R$ …(18)

(R =0.987, n = 8, *P* >95%)

(2*E*, 6*E*)-2,6-bis(substituted benzylidene) cyclohexanones

δH_β(ppm) = 7.596 (±0.200) + 0.010 (±0.430) σ_I – 0.529 (±0.953) σ_R …(19)

(R= 0.967, n = 9, *P* >96%)

δH_β(ppm) = 7.600 (±0.189) + 0.029 (±0.40) F – 0.524 (±0.358) R …(20)

(R=0.978, n = 9, *P* >94%)

(2*E*,6*E*)-2,6-bis(substituted benzylidene) cyclopentanones

δH_β(ppm) = 7.650 (±0.013) – 0.0216 (±0.040) σ_I – 0.092 (±0.056) σ_R …(21)

(R= 0.967, n = 9, *P* >95%)
δH_β(ppm) = 7.641 (±0.009) – 0.227 (±0.227) F – 0.135 (±0.033) R …(22)

(R=0.978, n = 9, ρ >93%)

^{13}C NMR spectral correlation study

The correlation analysis of the carbonyl carbon chemical shifts (ppm) for (1*E*,4*E*)-1,5-bis(substituted phenyl)penta-1,4-dien-3-ones did not yield satisfactory results with Hammett substituent constants, as well as F and R parameters (Supplementary Information, Table S1). However, a good correlation was observed for the C_α carbon chemical shifts (ppm) with σ, σ^+, and σ_R constants, all exhibiting positive ρ values. Similarly, the C_β carbon chemical shifts (ppm) displayed satisfactory correlation coefficients with σ_I, σ_R, F, and R parameters. The remaining correlations were found to be insignificant, which can be attributed to the factors discussed earlier and the resonance–conjugative structure illustrated in Fig. 2.

The correlation analyses of the CO, C_α, and C_β carbon chemical shifts (δ, ppm) for (2*E*,6*E*)-2,6-bis(substituted benzylidene)cyclohexanones exhibited satisfactory correlation coefficients with Hammett substituent constants, as well as F and R parameters, except for the H, 4-F, 4-CH_3, and 2-NO_2 substituents. However, the correlations based on the σ_R constants were found to be insignificant. This behaviour can be attributed to the factors discussed earlier and the resonance–conjugative structure depicted in Fig. 3.

The CO and C_β carbon chemical shifts (ppm) of (2*E*,6*E*)-2,6-bis(substituted benzylidene) cyclopentanones exhibited satisfactory correlation coefficients through the Hammett substituent constants (σ, σ^+, σ_I, σ_R) and R parameters, except for the 2-Cl, 4-F, 4-CH_3, and 4-OCH_3 substituents. The correlation of the C_α carbon chemical shifts (ppm) for these enones exhibited poor correlation coefficients, which may be attributed to the factors discussed earlier and the resonance–conjugative structural influence illustrated in Fig. 4.

Several single-parameter correlations failed to yield significant correlation coefficients for the spectral frequencies of the enones. However, the multiple regression analysis provided satisfactory correlation coefficients with the Swain–Lupton constants, as well as the F and R parameters[39]. The corresponding multi-regression equations are as follows (23–34).

(1*E*, 4*E*)-1,5-bis(substituted phenyl)penta-1,4-dien-3-ones

δCO(ppm) = 188.63 (±2.498) – 7.159 (±6.817) σ_I + 11.48 (±8.880) σ_R …(23)

(R =0.967, n = 7, *P* > 90%)
δCO(ppm) = 188.63 (±2.498) – 7.159 (±6.817) F + 11.48 (±8.880) R …(24)

(R =0.957, n = 7, *P* > 90%)
$\delta C\alpha$(ppm) = 128.09 (±0.952) –3.185 (±2.599) σ_I + 9.671 (±3.385) σ_R …(25)

(R =0.988, n = 7, *P* > 90%)
δC_α(ppm) = 128.24 (±2.060) – 1.747 (±2.798) F + 6.908 (±3.037) R …(26)

(R =0.993, n = 7, *P* > 90%)
δC_β(ppm) = 142.29 (±0.867) – 3.866 (±2.366) σ_I + 2.432 (±3.082) σ_R …(27)

(R =0.956, n = 7, *P* > 90%)

δC_β(ppm) = 141.90 (±0.881) – 3,284 (±2.405) F + 2.905 (±2.611) R …(28)

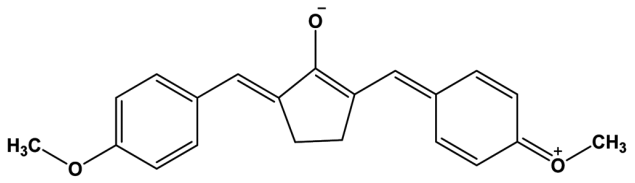

Fig. 4 — The methoxy substituted cyclohexanone based bis-enone

(R =0.965, n = 7, *P* > 90%)

$\delta CO(ppm) = 189.75\ (\pm 0.519) - 1.163\ (\pm 1.114)\ \sigma_I + 0.109\ (\pm 1.251)\ \sigma_R$ …(29)

(R =0.987, n = 7, *P* > 90%)

$\delta CO(ppm) = 189.67\ (\pm 0.528) - 0.528\ (\pm 0.743)\ F + 0.225\ (\pm 0.999)\ R$ …(30)

(R =0.945, n = 7, *P* > 90%)

$\delta C_\alpha(ppm) = 128.19\ (\pm 1.754) + 0.819\ (\pm 3.763)\ \sigma_I + 6.632\ (\pm 4.228)\ \sigma_R$ …(31)

(R =0.978, n = 7, *P* > 90)

$\delta C_\alpha(ppm) = 127.62\ (\pm 1.498) + 1.546(\pm 3.172)\ F + 5.990\ (\pm 4.228)\ R$ …(32)

(R =0.986, n = 7, *P* > 90%)

$\delta C_\beta(ppm) = 136.45\ (\pm 1.043) + 2.022\ (\pm 2.238)\ \sigma_I + 0.339\ (\pm 2.515)\ \sigma_R$ …(33)

(R =0.987, n = 7, *P* > 90%)

$\delta C_\beta(ppm) = 136.16\ (\pm 0.961) + 2.411\ (\pm 2.037)\ F + 0.606\ (\pm 1.820)\ R$ …(34)

(R =0.967, n = 7, *P* > 90%)

Docking analysis result

The molecular docking studies of bis-chalcone derivatives **1–13** were carried out with the human estrogen receptor (PDB ID: 3ERT), and the results revealed binding energy values within a comparable range. Among these, the compound (4,6-dihydropyren-2-yl)-5-(pyren-4-yl)penta-1,4-dien-3-one **13** exhibited the most favourable binding affinity, gives the binding energy of –9.18 kcal/mol. This ligand formed a hydrogen bond interactions with amino acid residues including CYS530 involving Cysteine; then hydrophobic interactions with amino acids residues such as LYS529, LEU525, TYR526, LEU536, and VAL533**,** involving Leucine, Lysine, Tyrosine, and Valine. The strong binding efficiency observed may be attributed to the presence of halogen substituents on the bis-chalcone framework. The corresponding 2D and 3D docking visualizations of the compound with the highest binding energy are presented in Table 3.

The molecular docking studies of bis-chalcone derivatives **14–29** were performed using the designed ligands against the target proteins. Among these, (2*E*,6*E*)-2,6-bis(2-chlorobenzylidene) cyclohexanone **16** and (2*E*,5*E*)-2,5-bis(4-meth-oxybenzylidene) cyclopentanone **28** exhibited the most favourable binding affinities, with docking scores of –6.87 and –6.31 kcal/mol, respectively. Both compounds demonstrated two hydrogen bonding interactions like CYS530, and MET522 involving cysteine, and methionine; then the prominent hydrophobic interactions with amino acid residues such as TRP383, LEU525, LEU536, VAL533, LYS529, and TYR526, along with additional contacts involving Tryptophan, Lysine, Tyrosine, Leucine, and Valine**.** The strong binding affinities observed may be attributed to the presence of halogen substituents in the molecular framework. The 2D and 3D docking visualizations illustrating the electrostatic and hydrophobic interactions of compounds **16** and **28** are presented in Table 3.

Based on these results, bis–chalcones **30–40** were docked with above said proteins. The bis-enone (2*E*, 2′*E*) -1,1′-(1,3-phenylene) bis(1-(4-chlorophenyl) prop-2-en-1-one) compound **32** was highest binding energy when compared to other compounds. Results pointed out that binding of all designed ligands displayed binding energy values with receptor protein **1M17** ranging from (–6.53 kcal/mol). The docking analysis revealed one electrostatic interactions including ARG849 involving Arginine, then the prominent hydrophobic interactions among the compound and specific amino acid residues together with ALA928, ILE886, LYS883, PHE731 and ALA730 along with additional interactions involving Alanine, Lysine, Isoleucine and Phenylalanine. The observed binding behaviour may be attributed to the influence of halogen substituents present in the compound. The corresponding 2D and 3D docking representations illustrating the electrostatic and hydrophobic interactions of compound **32** are provided in Table 3.

Based on these results, the bis–chalcones **41–54** were docked with above mentioned proteins. The bis-enone (2*E*,2*E*)-1,1′-(1,3-phenylene) bis(3-(4-methoxyphenyl) prop-2-en-1-one) compound **47** was highest binding energy when compared to other compounds. Results pointed out that binding of all designed ligands displayed binding energy values with receptor protein **1M17** ranging from (–7.85 kcal/mol). The docking analysis revealed two hydrogen bonding interactions including ILE854, and LYS855 involving Isoluecine, and Lysine then the prominent hydrophobic interactions among the compound and exact amino acid residues, including

Table 3 — The molecular docking protein binding interaction results of substituted bis–chalcone

Entry	2D docking pose	3D docking pose	Binding Energy ΔG (Kcal/mol)
13	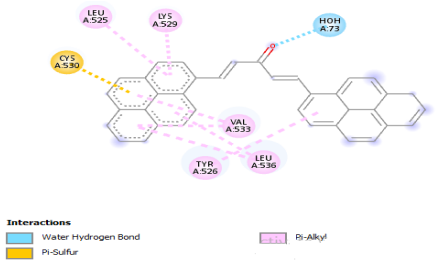	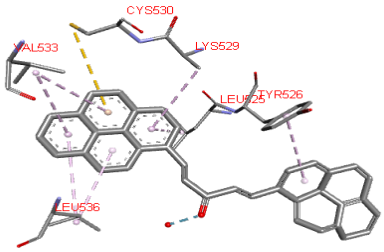	– 9.18
16	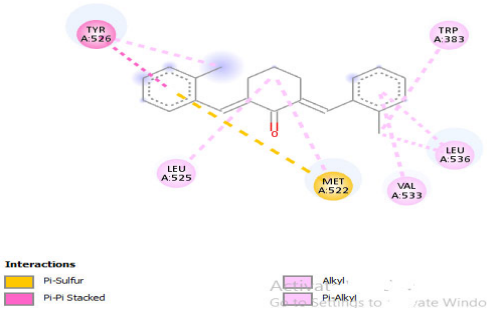	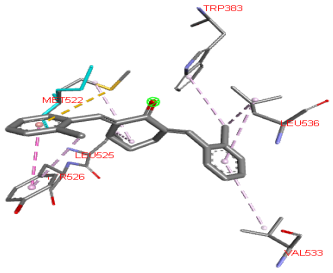	–6.87
28	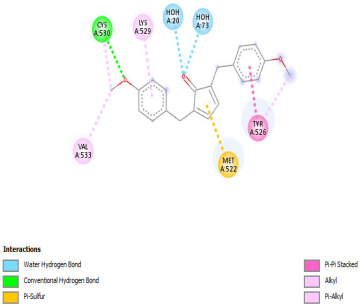	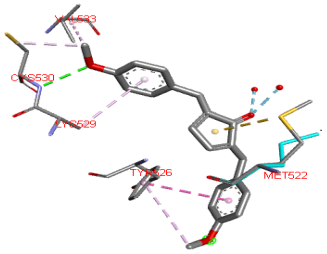	–6.31
32	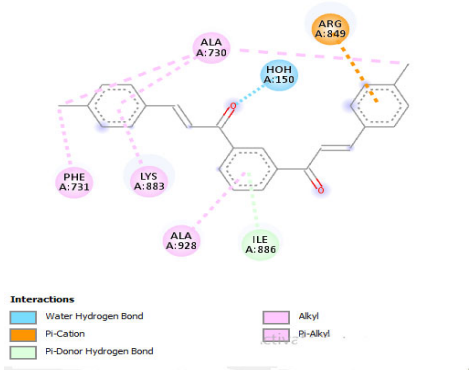	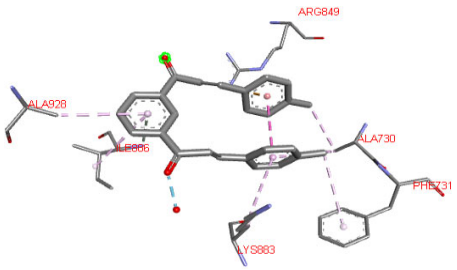	–6.53

(*Contd.*)

Table 3 — The molecular docking protein binding interaction results of substituted bis–chalcone (*Contd.*)

Entry	2D docking pose	3D docking pose	Binding Energy ΔG (Kcal/mol)
47	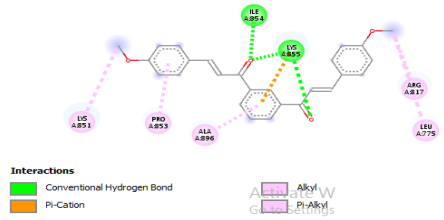	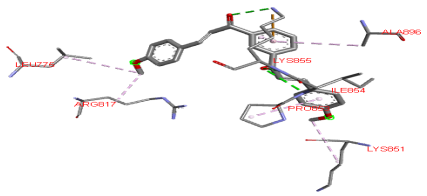	–7.85
56	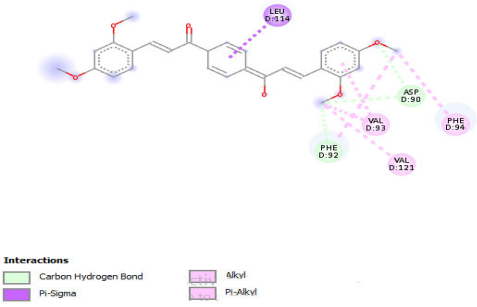	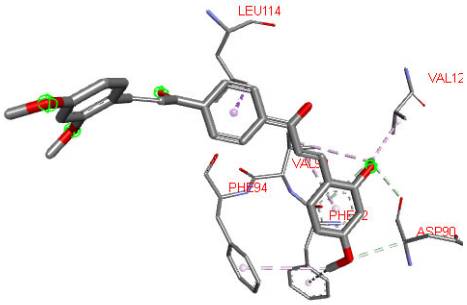	–8.01
58	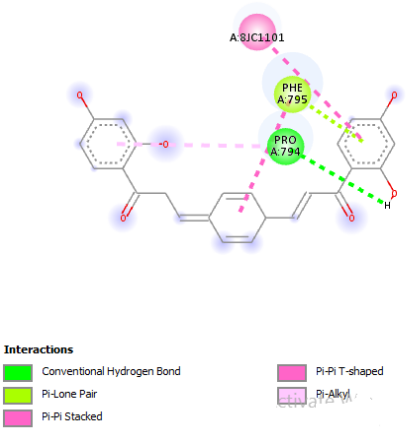	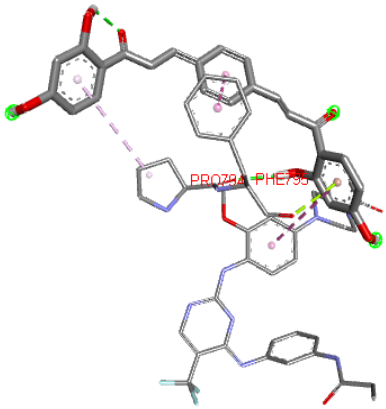	–5.82

ARG817, ALA896, LEU854, and PRO853, along with additional interactions involving Arginine, Alanine, Leucine and Proline residues. The observed binding efficiency may be attributed to the presence of halogen substituents within the bis-chalcone framework. The 2D and 3D docking visualizations illustrating the electrostatic and hydrophobic interactions of compound (**47**) are presented in Table 3.

Based on these results, the bis–chalcones **54**–**57** as ligands docked with above note proteins. The compound (2*E*,2'*E*)-1,1'-(1,4-phenylene) bis(3-(2,4-dihydroxy-phenyl)prop-2-en-1-one) **56** was highest binding energy when compared to other compounds. Results pointed out that binding of all designed ligands displayed binding energy values with receptor protein 5XDL ranging from (–5.82 kcal/mol). The docking analysis revealed one hydrogen bonding interactions including ASP90 it involving Aspartic acid and the prominent hydrophobic interactions among the compound and specific amino acid residues, together with PHE92, VAL93, VAL121, PHE94, along with additional interactions involving Valine and Phenylalanine residues. The 2D and 3D docking representations depicting the hydrogen bonding and hydrophobic interactions of compound **56** are provided in Table 3.

Based on these results, (1,4-phenyl Substituted Ketone bis–chalcone) (**58** and **59**) this designed ligands docked with the designed compounds were docked towards the colchicine binding site of Tubulin (1SA0). (2*E*,2'*E*)-1,1'-(1,4-phenylene) bis(3-(2,4-dimetho-xyphenyl)prop-2-en-1-one)compound **58** was highest binding energy when compared to other compounds. Results pointed out that binding of all designed ligands displayed binding energy values with receptor protein (1SA0) ranging from (–8.02 kcal/mol). The docking analysis revealed one hydrogen bonding interactions including PRO795 and involving Proline then the prominent hydrophobic interactions between the compound and specific amino acid residues, including PHE795 along with additional interactions involving Valine and Phenylalanine residues. The 2D and 3D docking representations depicting the hydrogen bonding and hydrophobic interactions. The observed docking behaviour may be attributed to the presence of halogen substituents within the bis-chalcone structure. The 2D and 3D docking visualizations depicting the electrostatic and hydrophobic interactions of compound **58** are presented in Table 3.

Antimicrobial activities

Antibacterial activity

Antibacterial activity was assessed through inhibition zone diameters (mm) values[40-45] from the petri-plates of chalcones is shown Table 4. The corresponding petri-plates and statistical column chart are illustrated in Fig. 5 and Fig. 6. In general, all bis–chalcone possess antibacterial activity against their bacterial microbes. Bis-enone **8, 9, 11, 12** are shown good and **10** and **13** shown moderate antibacterial activity toward *Staphylococcus aureus* strains. Here the +I effect of aryl rings enhances the antibacterial activity and the +I effect of chlorine and methoxy's group -I effect diminishes the antibacterial activity.

Table 4 — Antibacterial activities of the bis-enones **8-13**

Entry	R	Zone of Inhibition (mm)			
		Gram positive bacteria		Gram negative bacteria	
		S. aureus	*E. faecalis*	*E. coli*	*K. pneumonia*
8	9-Anthracenyl	23	22	24	25
9	4-Biphenyl	24	21	19	18
10	2, 3–Dichlorophenyl	19	20	18	19
11	2-Ferrocenyl	21	19	17	17
12	3–Methoxyphenyl	18	17	16	17
13	Pyrene–1–yl	20	19	18	20
Standard	Chloramphenicol	26	24	26	27

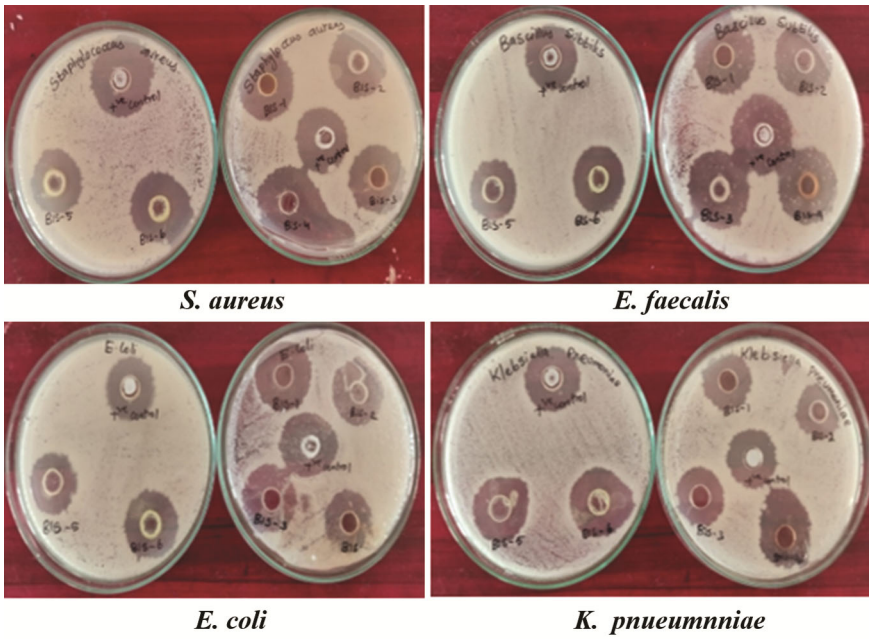

Fig. 5 — Petri-plates displays the antibacterial activities of bis enones **8-13**

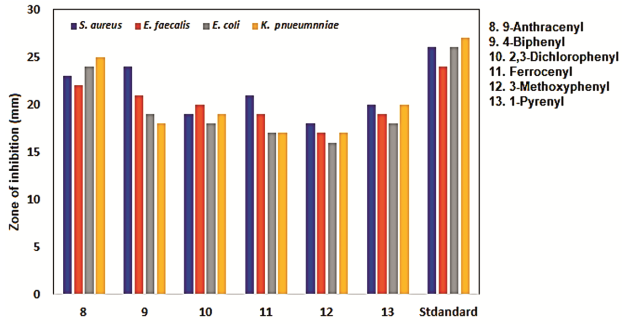

Fig. 6 — Antibacterial activities of bis enones **8-13** by means of statistical column chart

Table 5 — Antifungal activities of the bis-enones **8-13**

Entry	R	Zone of Inhibition (mm)	
		Candida albicans	*Candida auris*
8	9-Anthracenyl	18	20
9	4-Biphenyl	16	18
10	2,3-Dichlorophenyl	17	19
11	2-Ferrocenyl	8	17
12	3-Methoxyphenyl	13	14
13	Pyrene-1-yl	16	17
Standard	Fluconazole	20	22

Here the bis–chalcones and **8** and **10** and the remaining compounds shows good and moderate antibacterial activity against *Enterococcus faecalis* microbe. Here the +I effect of anthracene and chloride groups enhances the antibacterial activity. The remaining compounds shows moderate antibacterial activity. This can be attributed to the +I effect of aryl groups and methoxy's group -I effect unable to predict the antibacterial activity against the strain. The Bis-enone **9** show good antibacterial activity toward *Escherichia coli* bacterial organism. This is due to the enhancement of +I effect of anthracene moiety in the enones. The remaining compounds shows least activity and is associated with the weak +I effect of aryl, chloride and -I effect of methoxy substituents. The compounds **8** and **13** where exhibits good antibacterial activity toward *K. pneumonia strain*. Here the +I effect of anthracene and pyrene ring enhances the antibacterial activity. The other enones **9-12** shows moderate activity due to the inability of +I effect of aryl rings, chloride and the methoxy groups –I effect failed to justify the antibacterial results.

Antifungal activity

The antifungal activity profiles of the synthesized bis-chalcones, represented by their respective zone of inhibition measurements[40-45], are summarized in Table 5. The Petri plate and cluster column

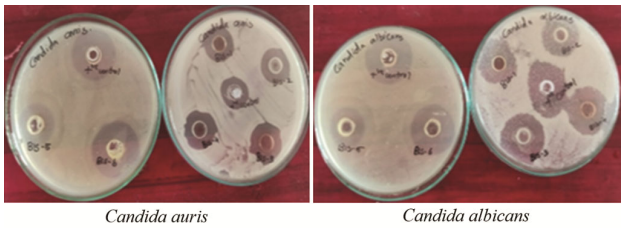

Fig. 7 — Antifungal activities of the bis-enones **8-13** by means of petri-plates

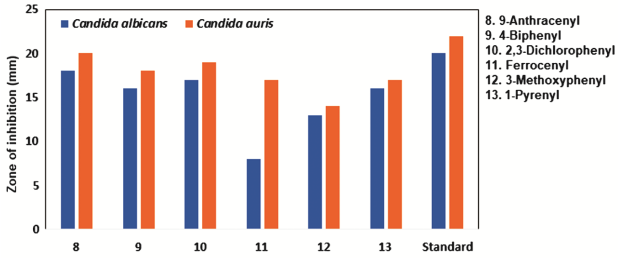

Fig. 8 — Antifungal activities of the bis-enones (**8-13**) by means of clustered column chart

representations depict the comparative antifungal responses of bis-enones **(8–13)** was presented in Fig. 7 and Fig. 8. In this study, all bis–chalcone active for showing their antifungal activity against their fungal microbes. All bis–chalcones except **11** and **12** are exhibits their good antifungal activity against *C. albicans* fungal microbe. Here the +I effect of aryl rings and chloride substituents enhances the antifungal activity. The least antifungal activity of above said enones is due to the incapable of +I effect of ferrocene and -I effect of methoxy substituents. Bis–chalcone **8-11** and **13** were shows good antifungal activities against *Candida auris* fungal strain. This is due to the +I effect of aryl rings and chloride substituents enhance the antifungal activity. The -I effect of methoxy substituent diminishes the antifungal efficacy against the strain.

Antimalarial activity

The measured antimalarial activity was presented in Table 6. The bromo and chloro and fluoro substituted bi-enones (**2-5** and **10**) shows better antimalarial activity than other aryl enones. The methoxy and ferrocene substituted enones also shows antimalarial activity than other enones with aryl substituents. Here the +I effect of chlorine enhances the antimalarial activity. The methoxy's group -I effect shows then ferrocene ring also shows moderate antimalarial activity. The remaining aryl rings such as phenyl, anthracene, biphenyl and pyrene have +I

Table 6 — Antimalarial activities of aryl bi-enones 8-13

Entry	R	Antimalarial activity
1	Ph	32±0.420
2	4-BrPh	38±0.435
3	2-ClPh	38±0.967
4	4-ClPh	37±0.991
5	4-FPh	36±0.187
6	4-OCH_3Ph	34±0.167
7	4-CH_3Ph	29±0.162
8	9–Anthracenyl	27±0.819
9	4-Biphenyl	29±0.900
10	2,3–Cl_2Ph	39±0.901
11	2-Ferrocenyl	31±0.702
12	3-OCH_3Ph	33±0.122
13	1-Pyrenyl	29±0.037

effect but they are not enhancing the antimalarial activity.

Experimental Section

Material and Methods

Reagents and solvents were obtained from Sigma-Aldrich and TCI Chemicals. The bis-chalcone's melting points were measured in open capillaries using a Raga Tech electrical melting point apparatus (uncorrected). FT-IR spectra (KBr, 3000–800 cm^{-1}) were documented on an Agilent Cary-630N spectrophotometer**.** ^1H (400 MHz) and ^{13}C (100 MHz) NMR spectra were documented in $CDCl_3$ with TMS as internal reference. Elemental analysis (CHN) was performed on a Perkin Elmer 240C analyzer.

General procedure for synthesis of bis-chalcones

Substituted benzaldehydes (2 mmol) and acetone (1 mmol), or aryl bis-aldehydes (1 mmol) with aryl ketones (2 mmol), were reacted in a 100 mL conical flask containing 0.3 mg of nano fly ash–H_3PO_4 catalyst[46] and 20 mL of ethanol, added in dropwise. The mixture was stirred at RT for 45 min (Scheme 2). Reaction progress was monitored by TLC. After completion, the mixture was poured into ice-cold water, and the precipitated product was filtered and dried. Recrystallization from ethanol yielded a pale-yellow crystalline solid. The percentage yields and physical properties are listed in Table 7.

The infrared, nuclear magnetic resonance and mass spectroscopic data of selective bis-enones are summarized.

(1*E*,4*E*)-1,5-Diphenylpenta-1,4-dien-3-one, 1

IR (KBr): 1654 ($CO_{s\text{-}cis\ cis}$), 1623 ($CO_{s\text{-}cis\ trans}$), 1613($CO_{s\text{-}trans\ trans}$), 3425 (CH), 1441 cm^{-1} (C=C); ^1H NMR (400 MHz, $CDCl_3$): δ 7.115(d, 2H, H_α),7.795 (d, 2H, H_β),7.284-7.655 (m, Ar-H, 10H); ^{13}C NMR (100 MHz, $CDCl_3$): δ 125.45 (C_α), 143.32 (C_β), 188.92(CO), 128.42-134.82(Ar-C); MS: *m/z* 434 [M^+].

(1*Z*,4*Z*)-1,5-Di(anthracen-9-yl) penta-1,4-dien-3-one, 8

IR (KBr): 1668 ($CO_{s\text{-}cis\ cis}$), 1627 ($CO_{s\text{-}cis\ trans}$), 1615($CO_{s\text{-}trans\ trans}$), 3427 (CH), 1441 cm^{-1} (C=C); ^1H NMR (400 MHz, $CDCl_3$): δ 7.982 (d, 2H, H_α), 8.919 (d, 2H, H_β),7.481to7.650 ppm (m, Ar-H, 21H); ^{13}C NMR (100 MHz, $CDCl_3$): δ 123.47 (C_α), 135.15 (C_β), 192.91 (CO), 123.47-135.15 (Ar-C); MS: *m/z* 434 [M^+].

(1*E*,4*E*)-1,5-Di([1,1'-biphenyl]-4-yl) penta-1,4-dien-3-one, 9

IR (KBr): 1660 ($CO_{s\text{-}cis\ cis}$), 1621 ($CO_{s\text{-}cis\ trans}$), 1603($CO_{s\text{-}trans\ trans}$), 3095(CH), 1487 cm^{-1} (C=C); ^1H NMR (400 MHz, $CDCl_3$): δ 6.763(d, 2H, H_α), 7.558 (d, 2H, H_β), 7.246 to 7.658 ppm (m, Ar-H,21H); ^{13}C NMR (100 MHz, $CDCl_3$): δ 126.99 (C_α), 143. 28 (C_β), 198.35 (CO), 126.99 -142.96 ;(Ar-C); MS: *m/z* 386[M^+].

(1*E*,4*E*)-1,5-bis(2,3-Dichlorophenyl) penta-1,4-dien-3-one, 10

IR (KBr): 1665($CO_{s\text{-}cis\ cis}$),1638 ($CO_{s\text{-}cis\ trans}$),1611($CO_{s\text{-}trans\ trans}$), 3036 (CH), 1509 cm^{-1} (C=C); ^1H NMR (400 MHz, $CDCl_3$): δ 6.644(d, 2H, H_α),7.924 (d, 2H, H_β),6.624 – 7.945 (m, Ar-H, 6H); ^{13}C NMR (100 MHz, $CDCl_3$): δ 125.76 (C_α),139.16 (C_β), 198.12(CO) 125.76-134.05 (Ar-C); MS: *m/z* 396 [M^+].

(1*E*,4*E*) -1,5-bis(Ferrocenyl)penta -1,4-dien-3-one, 11

IR (KBr): 1699($CO_{s\text{-}cis\ cis}$), 1640 ($CO_{s\text{-}cis\ trans}$), 1613 ($CO_{s\text{-}trans\ trans}$),3093 (CH), 1576 cm^{-1} (C=C_{op}); ^1H NMR (400 MHz, $CDCl_3$): δ 6.606 (d, 2H, H_α),7.625 (d,2H, H_β), 6.587–7.645(m, Ar-H, 10H); ^{13}C NMR (100 MHz, $CDCl_3$): δ 123.23 (C_α), 144.12 (C_β), 187.42 (CO), 123.23 –144.14 (Ar-C); MS: *m/z* 430 [M^+].

(1*E*,4*E*)-1,5-bis(3-Methoxyphenyl) penta-1,4-dien-3-one, 12

IR (KBr): 1656($CO_{s\text{-}cis\ cis}$), 1633 ($CO_{s\text{-}cis\ trans}$), 1602 ($CO_{s\text{-}trans\ trans}$), 3426 (CH),1574 cm^{-1} (C=C); ^1H NMR (400 MHz, $CDCl_3$): δ 6.604 (d, 2H, H_α), 7.697 (d, 2H, H_β),OCH_3(3.838), 6.584–7.717 (m, Ar-H, 8H); ^{13}C NMR (100 MHz, $CDCl_3$): δ 123.49 (C_α), 143.25 (C_β), 198.41 (CO) 126.82-143.46 (Ar-C); MS: *m/z* 294 [M^+].

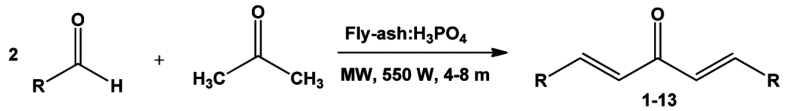

R= 1. Ph; 2. 4-BrPh; 3. 2-ClPh; 4. 4-ClPh; 5. 4-FPh; 6. 4-OCH_3Ph; 7. 4-CH_3Ph, 8. 9-Anthacene; 9. 4-Biphenyl; 10. 2,3-Cl_2Ph; 11. 2-Ferrocene; 12. 3-OCH_3Ph; 13. 1-Pyrene

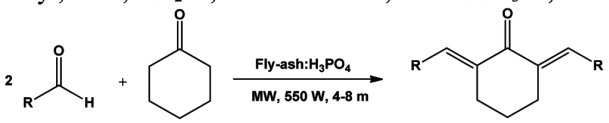

R= 14. Ph; 15. 4-BrPh; 16. 2-ClPh; 17. 4-ClPh; 18. 4-FPh; 19. 4-OHPh; 20. 4-OCH_3Ph; 21. 4-CH_3Ph; 22. 4-NO_2Ph

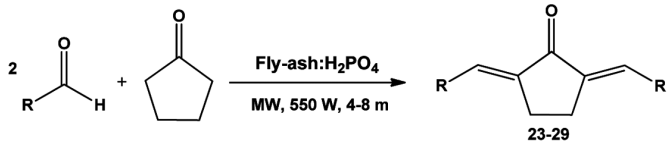

R= 23. Ph; 24. 4-BrPh; 25. 2-ClPh; 26. 4-ClPh; 27. 4-FPh; 28. 4-OCH_3Ph; 29. 4-CH_3Ph

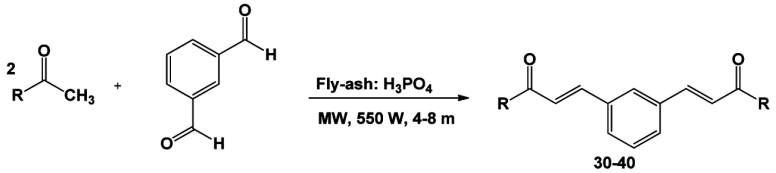

R= 30. Ph; 31. 4-BrPh; 32. 4-ClPh; 33. 4-FPh; 34. 2-Furyl; 35. 3,4–$(OCH_3)_2$Ph; 36. 4-OCH_3Ph; 37. 4-CH_3Ph; 38. 2-Thienyl; 39. 2,4–$(OCH_3)_2$Ph; 40. 2,4–$(OH)_2$Ph

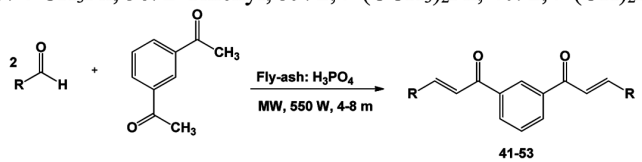

R= 41. Ph; 42. 4-BrPh; 43. 4-ClPh; 44. 4-FPh; 45. 2-Furyl; 46. 3,4–$(OCH_3)_2$Ph; 47. 4–(OCH_3)Ph; 48. 4–(CH_3)Ph; 49. 2-Thienyl; 50. 2,4–$(OCH_3)_2$Ph; 51. 2,4–$(OH)_2$Ph; 52. 3,4–$(OH)_2$Ph; 53. 4–OHPh

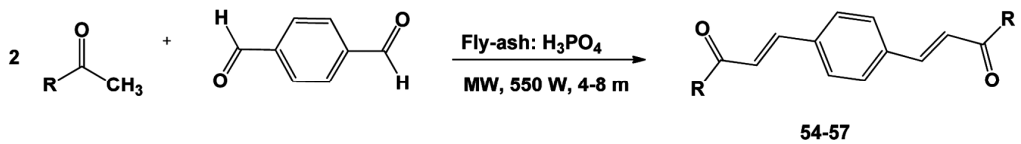

R= 54. 2,4–$(OCH_3)_2$Ph; 55. 3,4–$(OCH_3)_2$Ph; 56. 2,4–$(OH)_2$Ph; 57. 3,4–$(OH)_2$Ph;

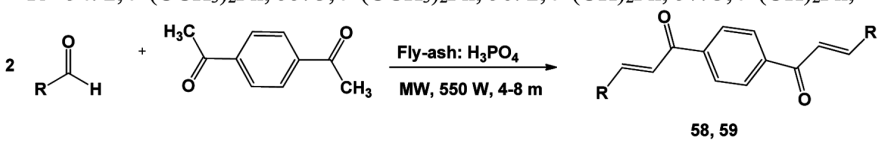

R= 58. 2,4–$(OCH_3)_2$Ph; 59. 2,4–$(OH)_2$Ph

Scheme 2 — Synthesis of bis-enones by Fly-ash:H_3PO_4 catalyzed Claisen-Schmidt condensation of various aryl ketones and aldehydes

Table 7 — The physical constants, analytical data and yields of bis-chalcones

Entry	Ketone/Aldehyde	R	Mol. Formula	Mol. Wt.	Yield (%)	m.p. (°C)
		(1*E*, 4*E*)-1,5-Bis(substituted phenyl)penta-1,4-dien-3-ones				
1	Acetone	Ph	$C_{17}H_{14}O$	234	60	113–115(110–115) (Ref. 47)
2	Acetone	4-BrPh	$C_{17}H_{12}Br_2O$	392	66	123–125(111–113) (Ref. 48)
3	Acetone	2-ClPh	$C_{17}H_{12}Cl_2O$	303	73	118–120(114–116) (Ref. 47)
4	Acetone	4-ClPh	$C_{17}H_{12}Cl_2O$	303	45	184–186(184–186) (Ref. 47)

(*Contd*.)

Table 7 — The physical constants, analytical data and yields of bis-chalcones (*Contd.)*

Entry	Ketone/Aldehyde	R	Mol. Formula	Mol. Wt.	Yield (%)	m.p. (°C)
5	Acetone	4-FPh	$C_{17}H_{12}F_2O$	270	74	150–154(150–152) (Ref. 47)
6	Acetone	4-OCH_3Ph	$C_{19}H_{18}O_3$	262	56	129–132(128–130) (Ref. 47)
7	Acetone	4-MePh	$C_{19}H_{18}O$	294	63	175-177(174 –176) (Ref. 47)
8	Acetone	9-Anthryl	$C_{33}H_{22}O$	434	78	167–169
9	Acetone	4-BiPh	$C_{29}H_{22}O$	386	88	187-189
10	Acetone	2,3-Cl_2Ph	$C_{17}H_{10}Cl_4O$	372	89	176-178
11	Acetone	2-Ferrocene	$C_{25}H_{19}Fe_2$	430	75	135-137
12	Acetone	3-OCH_3Ph	$C_{19}H_{18}O$	262	56	152-154
13	Acetone	1-Pyreneyl	$C_{37}H_{24}CO$	484	78	188-189
		(2*E*, 6*E*)-2,6-Bis(substituted benzylidene)cyclohexanones				
14	Cyclohexanone	Ph	$C_{20}H_{18}O$	274	64	116–118(116–120) (Ref. 47)
15	Cyclohexanone	4-BrPh	$C_{20}H_{16}Br_2O$	432	84	175-177(174-177) (Ref. 49)
16	Cyclohexanone	2-ClPh	$C_{20}H_{16}Cl_2O$	343	83	111–114(103–105) (Ref. 47)
17	Cyclohexanone	4-ClPh	$C_{20}H_{16}Cl_2O$	343	62	147–148(147–148) (Ref. 47)
18	Cyclohexanone	4-FPh	$C_{20}H_{16}F_2O$	310	36	154–157(154– 157) (Ref. 47)
19	Cyclohexanone	4–OHPh	$C_{20}H_{18}O_3$	306	67	167-168(166-168) (Ref. 50)
20	Cyclohexanone	4-OCH_3Ph	$C_{22}H_{22}O_3$	334	80	201–203(202–203) (Ref. 47)
21	Cyclohexanone	4–CH_3Ph	$C_{22}H_{22}O$	302	24	171-174 (170–171) (Ref. 47)
22	Cyclohexanone	4–NO_2Ph	$C_{20}H_{16}N_2O_5$	364	56	159(158–159) (Ref. 51)
		(2*E*, 6*E*)-2,6-Bis(substituted benzylidene)cyclopentanones				
23	Cyclopentanone	Ph	$C_{19}H_{16}O$	260	74	189–193(194–195) (Ref. 47)
24	Cyclopentanone	4–BrPh	$C_{19}H_{14}Br_2O$	418	69	192-193(191-194) (Ref. 32)
25	Cyclopentanone	2–ClPh	$C_{19}H_{14}Cl_2O$	329	82	158–160(155–158) (Ref. 47)
26	Cyclopentanone	4–ClPh	$C_{19}H_{14}Cl_2O$	329	80	225–228(227–229) (Ref. 47)
27	Cyclopentanone	4–FPh	$C_{19}H_{14}F_2O$	296	75	237–239(239–240) (Ref. 47)
28	Cyclopentanone	4–OCH_3Ph	$C_{21}H_{20}O_3$	320	64	215–217(210–211) (Ref. 47)
29	Cyclopentanone	4–CH_3Ph	$C_{21}H_{20}O$.	274	89	116–118(116–120) (Ref. 47)
		(2*E*, 2'*E*)-3,3'-(1, 3-Phenylene)bis(1-(substituted phenyl)prop-2-en-1-ones)				
30	Isophthaladehyde	Ph	$C_{24}H_{18}O_2$	338	56	140-141 (138–141) (Ref. 52)
31	Isophthaladehyde	4–BrPh	$C_{24}H_{16}Br_2O_2$	493	78	160-161(156–159) (Ref. 52)
32	Isophthaladehyde	4–ClPh	$C_{24}H_{16}Cl_2O$	407	95	135-136(133–137) (Ref. 52)
33	Isophthaladehyde	4–FPh	$C_{22}H_{16}F_2O$	374	79	157-159(155–158) (Ref. 52)
34	Isophthaladehyde	2-Furayl	$C_{26}H_{22}O_4$	318	67	148-150(146–148) (Ref. 52)
35	Isophthaladehyde	3,4–$(OCH_3)_2$Ph	$C_{28}H_{26}O_6$	458	76	167-168(166–168) (Ref. 52)
36	Isophthaladehyde	4–OCH_3Ph	$C_{26}H_{22}O_4$	398	88	124-126(123–125) (Ref. 52)
37	Isophthaladehyde	4–CH_3Ph	$C_{26}H_{22}O_2$	366	77	137-139(136–138) (Ref. 52)
38	Isophthaladehyde	2-Thienyl	$C_{20}H_{14}O_2S_2$	350	66	146-148(143–146) (Ref. 52)
39	Isophthaladehyde	2,4–$(OCH_3)_2$Ph	$C_{28}H_{26}O_6$	458	56	169-171(169–170) (Ref. 52)
40	Isophthaladehyde	2,4–$(OH)_2$Ph	$C_{28}H_{26}O_6$	458	56	166-168(169–170) (Ref. 52)
		(2*E*, 2'*E*)-1,1'-(1, 3-Phenylene)bis (3-(substitutedphenyl) prop-2-en-1-one)				
41	1,1'-(1,3-phenylene)diethanone	Ph	$C_{24}H_{18}O_2$	338	75	157-159(156–158) (Ref. 52)
42	1,1'-(1,3-phenylene)diethanone	4–BrPh	$C_{24}H_{16}Br_2O_2$	493	66	134-135(132–134) (Ref. 52)
43	1,1'-(1,3-phenylene)diethanone	4–ClPh	$C_{24}H_{16}Cl_2O$	407	78	146-148(145–147) (Ref. 52)
44	1,1'-(1,3-phenylene)diethanone	4–FPh	$C_{22}H_{16}F_2O$	374	65	154-156(151–154) (Ref. 52)
45	1,1'-(1,3-phenylene)diethanone	2-Furyl	$C_{26}H_{22}O_4$	318	76	170-172(169–171) (Ref. 52)
46	1,1'-(1,3-phenylene)diethanone	3,4–OCH_3Ph	$C_{28}H_{26}O_6$	458	74	168-170(166–169) (Ref. 52)
47	1,1'-(1,3-phenylene)diethanone	4–OCH_3Ph	$C_{26}H_{22}O_4$	398	56	179-181(177–179) (Ref. 52)
48	1,1'-(1,3-phenylene)diethanone	4–CH_3Ph	$C_{26}H_{22}O_2$	366	56	176-178(178–180) (Ref. 52)

(*Contd.)*

Table 7 — The physical constants, analytical data and yields of bis-chalcones (*Contd.)*

Entry	Ketone/Aldehyde	R	Mol. Formula	Mol. Wt.	Yield (%)	m.p. (°C)
49	1,1'-(1,3-phenylene)diethanone	2-Thienyl	$C_{20}H_{14}O_2S_2$	350	77	164-196(193–195) (Ref. 52)
50	1,1'-(1,3-phenylene)diethanone	2,4–$(OCH_3)_2$Ph	$C_{28}H_{26}O_6$	458	43	161-163(160–162) (Ref. 52)
51	1,1'-(1,3-phenylene)diethanone	2,4–$(OH)_2$Ph	$C_{24}H_{18}O_6$	402	31	139-141(138–140) (Ref. 52)
52	1,1'-(1,3-phenylene)diethanone	3,4–$(OH)_2$Ph	$C_{24}H_{18}O_6$	402	61	233-235(236–237) (Ref. 52)
53	1,1'-(1,3-phenylene)diethanone	4-OHPh	$C_{24}H_{18}O_4$	369	77	272-274(271–273) (Ref. 52)
		2*E*,2'*E*)-3,3'-(1,4-Phenylene)bis(1-(substituted phenyl)prop-2-en-1-ones)				
54	Terephthalaldehyde	2,4–$(OCH_3)_2$Ph	$C_{28}H_{26}O_6$	458	60	216-218(215–217) (Ref. 28)
55	Terephthalaldehyde	3,4–$(OCH_3)_2$Ph	$C_{28}H_{26}O_6$	458	63	229-231(231–232) (Ref. 28)
56	Terephthalaldehyde	2,4-$(OH)_2$Ph	$C_{24}H_{18}O_6$	402	65	249-251(252–254) (Ref. 28)
57	Terephthalaldehyde	3,4-$(OH)_2$Ph	$C_{24}H_{18}O_6$	402	63	154-157(156–159)) (Ref. 28)
58	1,1'-(1,4-phenylene)diethanone	2,4–$(OCH_3)_2$Ph	$C_{28}H_{26}O_6$	458	60	218-221(220–221) (Ref. 28)
59	1,1'-(1,4-phenylene)diethanone	2,4-–$(OH)_2$Ph	$C_{24}H_{17}O_6$	402	78	228-230(227–228) (Ref. 28)

(1*E*,4*E*)-1-(4,6-Dihydropyren-2-yl)-5-(pyren-4-yl) penta-1,4-dien-3-one, 13

IR (KBr): 1665($CO_{s\text{-}cis\ cis}$),1638 ($CO_{s\text{-}cis\ trans}$),1611 ($CO_{s\text{-}trans\ trans}$), 3036 (CH),1509 cm^{-1} (C=C); ^1H NMR (400 MHz, $CDCl_3$): δ 7. 003 (d, 2H, H_α), 8.667 (d, 2H, H_β), 8.027 to 8.459 (m, Ar-H, 17H); ^{13}C NMR (100 MHz, $CDCl_3$): δ 123. 03 (C_α),139.79 (C_β), 198.12 (CO), 124.12– 139.71(Ar-C); MS: *m/z* 484[M^+].

Molecular Docking study

The anticancer potential of the synthesized compounds was evaluated through molecular docking with AutoDock 4.2[31-34]. Docking simulations were carried out to examine the ligand–protein interactions at the active sites of the selected receptor (PDB ID: 3ERT), chosen for its high-resolution structure and well-defined binding pocket. The interaction profiles revealed hydrogen bonding, π–π stacking, and van der Waals forces, indicating significant binding affinity toward the receptor. The docking results, comprising binding energies and amino acid interactions. The ligand structures were initially designed in CDX format using ChemDraw Ultra (version 7.0) and subsequently converted to PDB format for docking analysis. A stepwise protocol was employed to prepare the receptor and ligands. Polar hydrogens and Kollman charges were added to the estrogen receptor alpha (ERα), while Gasteiger charges were assigned to all selected ligands to optimize their electrostatic states. The grid box was configured to dimensions of 60×60×60 points, centred at the binding site coordinates (x = 30.282, y = −1.913, z = 24.207) with a grid spacing of 0.375 Å. During the docking simulations, ERα was treated as a rigid receptor, whereas all ligands were considered flexible, allowing optimal conformational adaptation within the binding pocket. The genetics algorithm run was set to 100, and the Lamarckian genetic was chosen to proceed with the docking, while the other parameters were left as default. Docking scores were determined using the Discovery Studio Visualizer. This demonstrates the binding sites, hydrogen bonding interactions, hydrophobic interactions, and bond lengths. Binding energy (ΔG) is a vital parameter that provides information about the strength of binding energy indicates good interaction amongst the ligand and protein. The binding energy values of compounds **(1-59)** was given in Table S2 (Supplementary Information, Table S2).

Antimicrobial activities

Analysis of antibacterial sensitivity assay

The antibacterial susceptibility assay was performed by means of the Kirby–Bauer disc diffusion method[40]. Two Gram-positive and two Gram-negative bacterial strains *Staphylococcus aureus*, *Enterococcus faecalis*, *Escherichia coli*, and *Salmonella typhi* were employed to evaluate the antibacterial potential of the synthesized bis-chalcones **(8–13)**. Approximately 0.5 mL of the bacterial inoculum was evenly spread over the solidified Mueller–Hinton agar surface using a sterile

glass spreader. Sterile Whatman No. 1 filter paper discs (5 mm diameter) impregnated with the test compound solutions were carefully placed on the agar surface using sterile forceps. These plates were incubated at 37 °C for 24 h to prevent condensation on the agar surface. After incubation, the inhibition zone's diameters were measured, and the experiments were conducted in triplicate to ensure reproducibility.

Analysis of antifungal sensitivity assay

The antifungal susceptibility assay was conducted by means of the Kirby–Bauer disc diffusion method[41]. The antifungal efficacy of the synthesized bis-chalcones **(8–13)** was evaluated against two fungal strains, namely *Candida albicans* and *Candida tropicalis*. The potato dextrose agar (PDA) medium was arranged and sterilized following the same procedure described previously. Approximately 1 mL of the fungal inoculum was uniformly distributed over the solidified medium by gently rotating the Petri plate in both clockwise and counter clockwise directions to ensure even spreading. The test solution was prepared by dissolving 15 mg of sulfonamide derivatives in 1 mL of DMSO. The plates were then allowed to solidify for 24 h, after which the diameters of the inhibition zones were measured. All experiments were performed in triplicate to confirm reproducibility and accuracy of the results.

Analysis of antimalarial activities

Parasite Culture

The *Plasmodium falciparum* Thailand strain (Thai) and strain K1 were employed for the *in vitro* antimalarial assay[11]. Parasites were cultured in RPMI-1640 medium supplemented with 11 mM glucose, 27.5 mM sodium bicarbonate, 100 U/mL penicillin, 100 μg/mL streptomycin, and 8% of heat-inactivated human serum albumin. Cultivation was carried out at 37 °C using A^+ human red blood cells at a 2% hematocrit, under a controlled gas mixture of 3% CO_2, 6% O_2, and 91% N_2. Parasitemia levels ranging between 3–6% were maintained. The parasite density was evaluated microscopically using Giemsa-stained thin smears.

Inhibition Assay

A series of increasing concentrations of the synthesized amine derivatives was dissolved in dimethyl sulfoxide (DMSO) and evaluated for their inhibitory effects on the intraerythrocytic growth of *P. falciparum*.

Parasite Growth and Inhibition Assay

Parasite cultures were incubated at 37 °C for 24 h in a candle jar environment, after which 0.5 μCi of [^{3}H]-hypoxanthine was added to each well. Following a further 24 h incubation, the cultures were freeze-thawed and harvested onto glass fibre filters. The dried filters were then soaked in scintillation fluid, and the radioactivity was quantified using a 1450 MicroBeta scintillation counter. The percentage of growth inhibition was calculated based on the reduction in parasite-associated radioactivity relative to the untreated control, which represented 100% [^{3}H]-hypoxanthine incorporation. The half-maximal inhibitory concentration (IC_{50}) for each test compound was determined from three independent experiments by nonlinear regression analysis of log concentration *versus* percentage inhibition, performed using GraphPad Prism. The antimalarial potential of the synthesized imine derivatives was subsequently interpreted from the derived IC_{50} values.

Conclusions

A total of fifty-nine substituted bis-enones belonging to seven different series were synthesized with yields exceeding 60% *via* a nano–Fly-ash: H_3PO_4-catalyzed Claisen–Schmidt condensation between various aryl diketones and aldehydes under conventional conditions. The purity of the obtained enones was confirmed through their physical constants and spectroscopic data, which were found to be consistent with previously reported literature values. Statistical correlation analysis of the νC=O and νC=C stretching frequencies (cm^{-1}) for bis-chalcones (1*E*,4*E*)-1,5-bis(substituted phenyl)penta-1,4-dien-3-ones with Hammett substituent constants (σ, σ^+, σ_R) and resonance (R) parameters revealed satisfactory linear relationships, except in the case of methyl and methoxy substituents. Similarly, for (2*E*,6*E*)-2,6-bis(substituted benzylidene) cyclo-hexanones, the νC=O (cm^{-1}) stretching frequencies exhibited strong correlation by means of Hammett constants, while the νC=C (cm^{-1}) vibrations demonstrated reliable relationships with resonance and field components, excluding the bromo-substituted derivatives. The inductive influence of substituents in (1*E*,4*E*)-1,5-bis(substituted phenyl) penta-1,4-dien-3-ones exhibited a significant correlation with the H_α proton chemical shifts (ppm), except for the hydrogen and methyl-substituted derivatives, which deviated from the expected trend. The H_β proton chemical shifts (δ, ppm) of (2*E*,6*E*)-2,6-bis(substituted benzylidene)-

cyclohexanones showed satisfactory correlation coefficients with the Hammett substituent constants (σ), field (F), and resonance (R) parameters, except for the hydrogen substituent in the σ_i and F correlations. Furthermore, the C_α carbon chemical shifts (ppm) of (1*E*,4*E*)-1,5-bis(substituted phenyl) penta-1,4-dien-3-ones displayed a positive ρ value and a strong correlation with σ, σ^+, and σ_R substituent constants, confirming the electronic influence of the substituents. Similarly, the C_β carbon chemical shifts (δ, ppm) exhibited notable linear relationships with σ_I, σ_R, F, and R parameters, indicating the combined effects of inductive and resonance interactions on the electronic environment of the carbon framework. The C=O, C_α, and C_β carbon chemical shifts (δ, ppm) of (2*E*,6*E*)-2,6-bis(substituted benzylidene)cyclohexanones exhibited satisfactory correlation coefficients with the Hammett substituent constants (σ), field (F), and resonance (R) parameters, except in the cases of H, 4-F, 4-CH_3, and 2-NO_2 substituents. Similarly, the C=O and C_β carbon chemical shifts (δ, ppm) of (2*E*,6*E*)-2,6-bis (substituted benzylidene) cyclopentanones displayed good linear correlations with σ, σ^+, σ_I, σ_R, and R parameters, excluding 2-Cl, 4-F, 4-CH_3, and 4-OCH_3 derivatives. The multi-regression analyses of these spectral frequencies further confirmed statistically satisfactory correlations, indicating reliable substituent–chemical shift relationships. Molecular docking studies revealed that enones **13, 16, 28, 32, 47, 56,** and **58** demonstrated strong protein–ligand binding affinities, signifying promising bio-interactions. From the antimicrobial activity evaluations, enones **8–11** exhibited notable antibacterial efficacy against the tested microbial strains, whereas all bis-chalcones, except compounds **11** and **12**, displayed potent antifungal effects. Furthermore, halogen-substituted bis-enones exhibited enhanced antimalarial activity compared to their non-halogenated counterparts.

Supplementary Information

Statical analysis, molecular docking analysis results, mechanistic pathways and NMR spectra of selective bis-enones are available. Supplementary information is available in the website http://nopr.niscpr.res.in/handle/123456789/58776.

Acknowledgement

Two authors (P. Gayathri and Dr. G. Thirunarayanan) express their thanks to RUSA-2, Field 1, Anti-Malarial Drug Synthesis, No. F3/RUSA/673/2022 dated 4-6-2022, Annamalai University, Annamalainagar 608 002.

References

1 Liabadi R S, Mahmoodi NO, Ghafoori H, Roohi H & Pourghasem V, *Res Chem Intermed*, 44 (2018) 2999.
2 Raju K, Vinod J & Mulukuri S, *Int J Res Pharm Chem*, 7 (2017) 585.
3 Durgapal S D, Soman S S, Umar S & Balakrishnan S, *Synth Comm*, 50 (2020) 2502.
4 Husain A, Javed S, Mishra R, Rashid M & Bhutani R, *Pharmacophore*, 2 (2011) 280.
5 Go M L, Wu X & Liu X L, *Curr Med Chem*, 12 (2005) 483
6 Iwata S, Nishino T, Inoue H, Nagata N, Satomi Y & Nishino H, *Biol Pharm Bull*, 20 (1997)1266.
7 Prabhudev S M, Sultana S, Singh K Kallur H J & Yasmeen B, *World J Phar Res*, 9 (2020) 1445.
8 Siddiqui Z N & Khan T, *J Braz Chem Soc*, 25 (2014) 1002
9 Gajbhiye J M & Jamode V S, *Asian J Chem*, 13 (2001) 363.
10 Gomha S M, Edrees M M & Altalbawy F M A, *Int J Mol Sci*, 17 (2016). (https://doi.org/10.3390/ijms17091499).
11 Gurdere M B, Ozbek O & Ceylan M, *Synth Comm*, 46 (2016) 322.
12 Nagaraj A &Sanjeeva Reddy C, *Iran J Chem Soc*, 5 (2008) 262.
13 Ganesan R, Avupati VR & Shabi M M, *Indo Am J Pharm Sci*, 4 (2017) 670.
14 Arslan T, Celik G, Celik H, Senturk M, Yayli N & Ekinci D, *Arch Pharm*, 349 (2016) 741.
15 Thirunarayanan G, *Indian J Chem*, 46B (2007) 1511.
16 Gaonkar S L & Vignesh U N, *Res Chem Intermed*, 43 (2017) 6043.
17 Farooq S & Ngaini Z, *Curr Org Cat*, 6 (2019) 184.
18 Burmaoglu S, Gobek A, Aydin B O, Yurtoglu E, Aydin B N, Ozkat G Y, Hepokur C, Ozek N S, Aysin F, Altundas R & Algul O, *Bioorg Chem*, 111 (2021) 104882.) https://doi.org/10.1016/j.bioorg.2021.104882).
19 Jung C, Lee Y, Min D, Jung M & Oh S, *Molecules*, 22 (2017) 1872.
20 Arulkumaran R, Vijayakumar S, Sundararajan R, Sakthinathan S P, Kamalakkannan D, Suresh R, Ranganathan K, Vanangamudi G & Thirunarayanan G, *Int Lett Chem Phys Astro*, 4 (2012) 17.
21 Pereira R, Silva A M S, Ribeiro D, Silva V L M & Fernandes E, *Euro J Med Chem*, 252 (2023) 115280. http://dx.doi.org/ 10.1016/j.ejmech.2023.115280
22 Jose N, Domínguez N, Rodrigues J, María Eugenia Acosta A M, Caraballo N & León C, *J Enzym Inhibit Med Chem*, 28 (2012) 1267.
23 Raj C G D, Sarojini B, Bhanuprakash V, Yogisharadhya R, Kumar Swamy B E & Raghavendra R, *Med Chem Res*, 21 (2011) 2671.
24 Burmaoglu S, Ozcan S, Balcioglu S, Gencel M, Noma S A, Essiz S, Ates B & Algul O, *Bioorg Chem*, 91 (2019) 103149.
25 Tala-Tapeh S M, Mahmoodi N O & Vaziri A, *Bull Appl Res Sci*, 4 (2014) 63.
26 Polo E, Ibarra-Arellano N, Prent-Penaloza L, Morales-Bayuelo A, Henao J, Galdamez A & Gutierrez M, *Bioorg Chem*, 90 (2019) 103034.
27 Vanangamudi G, Subramanian M & Thirunarayanan G, *Arabian J Chem*, 10 (2017) S1254.

28 Cai C Y, Rao L, Rao L Y, Guo J X, Xiao Z Z, Cao J Y, Huang Z S & Wang B, *Eur J Med Chem*, 130 (2017) 51.

29 Wang Y, Curtis-Long M J, Lee B W, Yuk H J, Kim D W, Tan X F & Park K H, *Bioorg Med Chem*, 22 (2014) 1115.

30 Muthuvel I, Dineshkumar S, Thirumurthy K, Krishnakumar B & Thirunarayanan G, *Indian J Chem*, 55B (2016) 252.

31 Insuasty D, García S, Abonia R, Insuasty B, Quiroga J, Nogueras M, Cobo J, Borosky G L & Kenneth K, *Arch Pharm*, 354 (2021) e2100094.

32 Wei X, Du Z, Zheng X, Cui X, Conney A H & Zhang K, *Euro J Med Chem*, 53 (2012) 235.

33 Syahri U, Yuanita E, Nurohmah B A, Armunanto R & Purwono B, *Asian Pacific J Trop Biomed*, 7 (2017) 675.

34 P Gayathri, J Divya, I Muthuvel, V Usha, Malar Retna & G Thirunarayanan, *Indian J Chem*, 64 (2025) 670.

35 Mayavel P, Divya J, Gayathri P, Balasundari S, Usha V, Muthuvel I, Krishnakumar B, Shivakumara K N, Gurusamy R & Thirunarayanan G, *Res Chem Intermed*, 50 (2024) 4503.

36 Malar Retna A, Muthuvel I, Usha V & Thirunarayanan G, *Indian J Nat Sci*, 15 (2024) 76584.

37 Nalini S, Muthuvel I & Thirunarayanan G, *Indian J Nat Sci*, 14 (2023) 60659.

38 Kamalakkannan D, Senbagam R, Vanangamudi G & Thirunarayanan G, *J Mol Struct*, 1264 (2022) 133218.

39 Swain C G & Lupton E C J, *J Am Chem Soc*, 90 (1968) 4328.

40 Bauer A W, Kirby W M M, Sherris J C & Truck M, *Am J Cli Pathol,* 45 (1996) 493.

41 Venkatraman R, Divya J, Gayathri P, Muthuvel I & Thirunarayanan G, *Indian J Chem*, 64(2025) 465.

42 Gayathri P, Muthuvel I, Mayavel P, Ranganathan K, Usha V, Mala V & Thirunarayanan G, *Ovidius Univ Annal Chem*, 36 (2025) 66.

43 Muthuvel I, Divya J, Gayathri P, Balasundari S, Sudha P, Palanivel C, Krishnakumar C, Manikandan V, Alanazi A K & Thirunarayanan G, *Indian J Chem*, 64 (2025) 942.

44 Muthuvel I, Manikandan S, Thirunarayanan G, Usha V & Sathiyendiran V, *Indian J Chem*, 62 (2023) 131.

45 Usha V, Thirunarayanan G & Manikandan S, *Indian J Chem*, 61 (2022) 521.

46 John Joseph S, Ranganathan K, Suresh R, Arulkumaran R, Sundararajan R, Kamalakkannan D, Sakthinathan S P, Vanangamudi G, Dineshkumar S, Thirumurthy K, Muthuvel I, Thirunarayanan G & Viveksarathi V, *Mat Sci Appl Chem*, 34 (2017)12.

47 Silva C C D, Pacheco B S, Neves R N D, Alves M S D, Lopes A S, Moura S, Sibele B & Pereiraa C M P D, *Bio Pharm*, 111 (2019) 367.